Condensed complexes, rafts, and the chemical activity of cholesterol in membranes

Arun Radhakrishnan, Thomas G. Anderson, and Harden M. McConnell*

Department of Chemistry, Stanford University, Stanford CA 94305

Contributed by Harden M. McConnell, August 31, 2000

Epifluorescence microscopy studies of mixtures of phospholipids and cholesterol at the air–water interface often exhibit coexisting liquid phases. The properties of these liquids point to the formation of ''condensed complexes'' between cholesterol and certain phospholipids, such as sphingomyelin. It is found that monolayers that form complexes can incorporate a low concentration of a ganglioside G_{M1}. This glycolipid is visualized by using a fluorescently labeled B subunit of cholera toxin. Three coexisting liquid phases are found by using this probe together with a fluorescent phospholipid probe. The three liquid phases are identified as a phospholipid-rich phase, a cholesterol-rich phase, and a condensed complex-rich phase. The cholera toxin B labeled ganglioside G_{M1} is found exclusively in the condensed complex-rich phase. Condensed complexes are likely present in animal cell membranes, where they should facilitate the formation of specialized domains such as rafts. Condensed complexes also have a major effect in determining the chemical activity of cholesterol. It is suggested that this chemical activity plays an essential role in the regulation of cholesterol biosynthesis. Gradients in the chemical activity of cholesterol should likewise govern the rates and direction of intracellular intermembrane cholesterol transport.

monolayers | liquid phase separations | phospholipids | sphingomyelin

The physical properties of mixtures of cholesterol, phospholipids, and glycosphingolipids must play important roles in the regulation of their synthesis, transport, and localization in animal cell membranes. These properties determine the nature of the liquid bilayer regions of the membranes. Bilayers in animal cell membranes are far from ideal liquids. Even binary mixtures of cholesterol and phospholipids in bilayers are nonideal (1). Striking deviations from ideality are also observed in monolayer mixtures at the air–water interface (2–6). These include deviations from ideal mixing for average molecular areas, pairs of upper miscibility critical points (7, 8), and remarkable electric field-induced phase separations (9). In recent work, it has been found that these nonideal thermodynamic properties can be approximated theoretically in terms of a quantitative model of the liquid state of the membrane involving "condensed complexes" of cholesterol with specific phospholipids (8, 10). This liquid-state model is, in some respects, related to earlier theoretical work on cholesterol containing bilayers (11–13), but differs in that it involves a specific stoichiometric reaction with a finite equilibrium constant. The model predicts three liquid phases. The model is closely related to general theories of reactive liquid mixtures given by Corrales and Wheeler (14) and by Talanquer (15).

There is substantial indirect evidence that points to the presence in cell membranes of distinct lipid regions termed ''rafts,'' which are rich in sphingolipids and cholesterol (16–20). They are reported to be important for cellular functions such as signal transduction (20–23) and the sorting and transport of lipids and proteins (24–27). It has occurred to us that the lipid component of rafts may be largely composed of cholesterol-phospholipid complexes. This led us to label these complexes in monolayers by using one of the fluorescent techniques used to identify rafts in cell membranes, namely the tagging of a ganglioside G_{M1} (GM1) that is thought to be exclusively found in rafts (28). The tag is a fluorescently labeled B subunit of cholera toxin (CT-B). We find that in monolayers containing cholesterol, phospholipids, and GM1, only one of three coexisting liquid phases is labeled by CT-B. This phase is identified as the condensed complex-rich phase. As discussed below, the other two phases in the monolayers are a phospholipid-rich phase and a cholesterol-rich phase.

In addition to the suggested relation between condensed complexes and rafts, there are other aspects of the physical chemistry of complexes that appear relevant to animal cell membranes. Complexes have a large effect on the relation between membrane composition and the chemical activity of cholesterol. In monolayers, there is both experimental and theoretical evidence of a strong, almost step-like increase of cholesterol chemical activity on increasing cholesterol concentration beyond the complex stoichiometric composition (29). The binding of membrane cholesterol to specific proteins likely depends on this chemical activity.

To understand better the role of complexes in regulating membrane properties, we have extended the liquid state model (8, 10) to a ternary mixture of cholesterol C, and two lipids, S and U. S refers to lipids such as sphingomyelins or phosphatidylcholines with long saturated fatty acid chains that form complexes with cholesterol. These complex forming lipids typically have high T_m values (30), where T_m is the chain melting transition temperature. U is a lipid such as a phosphatidylcholine with unsaturated fatty acid chains that does not form complexes. Phosphatidylcholines with short saturated fatty acid chains also do not form complexes. These noncomplex forming lipids typically have lower T_m values (30). S and U alone are assumed to mix ideally.

C and S undergo a reversible reaction to form a complex:

$$nq\mathrm{C} + np\mathrm{S} \leftrightarrow \mathrm{C}_{nq}\mathrm{S}_{np} \qquad [1]$$

Here, n is an oligomerization (cooperativity) parameter and q and p are relatively prime stoichiometry integers. In the model, there are four molecular species in the liquid membrane, but only three independent chemical components. Many but not all reported phase diagrams conform to $q = 1$ and $p = 2$, with n ranging from 1 to as large as 10 (8, 9).

Materials and Methods

Model Calculations. The free energy for this reactive ternary mixture model is:

$$G = NkT \sum_i x_i \ln x_i + NkT_r \sum_{i<j} a_{ij} x_i x_j + N \sum_i x_i \mu_i^0 \qquad [2]$$

Abbreviations: GM1, ganglioside G_{M1}; DChol, dihydrocholesterol; DMPS, dimyristoylphosphatidylserine; DMPC, dimyristoylphosphatidylcholine; DPPC, dipalmitoylphosphatidylcholine; F-DHPE, fluorescein dihexadecanoyl phosphoethanolamine; Alexa, Alexa Fluor™ 594; CT-B, B subunit of cholera toxin; β-CD, β-cyclodextrin.

*To whom reprint requests should be addressed. E-mail address: harden@stanford.edu.

The publication costs of this article were defrayed in part by page charge payment. This article must therefore be hereby marked "*advertisement*" in accordance with 18 U.S.C. §1734 solely to indicate this fact.

Article published online before print: *Proc. Natl. Acad. Sci. USA*, 10.1073/pnas.220418097. Article and publication date are at www.pnas.org/cgi/doi/10.1073/pnas.220418097

N is the equilibrium number of molecules in the sample; x_i and μ_i^0 are, respectively, the mole fractions and standard chemical potential of the four species, C, S, U, and $C_{nq}S_{np}$. The a_{ij} are energy parameters representing a mean field "repulsion" between the several molecular pairs, normalized with respect to kT_r, where T_r is a reference temperature chosen to be room temperature. Diagonal (a_{ii}) and higher order terms are omitted for simplicity. These energy parameters depend on the surface pressure π of the monolayer according to $a_{ij} = 2 + a'_{ij}(\pi_{ij} - \pi)$, where the π_{ij} are the critical pressures of hypothetical binary mixtures of i and j. The a'_{ij} have units of reciprocal surface pressure. The standard chemical potential of the complex, $\mu^0_{C_{nq}S_{np}}$, is related to the standard chemical potentials through the equilibrium constant for the reaction (Eq. **1**), by $\mu^0_{C_{nq}S_{np}} = np\mu^0_C + nq\mu^0_S - kT_r \ln K_{eq}$. The equilibrium constant varies with the surface pressure according to $K_{eq} = K^0_{eq} \exp(-\pi\Delta A/kT_r)$, where K^0_{eq} is the equilibrium constant of the reaction at a reference surface pressure of $\pi = 0$, and ΔA is the area change of reaction. The mole fractions x_i are determined by the extent of reaction (Eq. **1**), $\xi = N_{C_{nq}S_{np}}/N_0$, where N_0 is the number of molecules present if no reaction occurs. The free energy (Eq. **2**) was minimized with respect to ξ to obtain the composition and free energy at chemical equilibrium.

Monolayer Experiments. Egg sphingomyelin (egg-SM), dimyristoylphosphatidylcholine (DMPC), dimyristoylphosphatidylserine (DMPS), dipalmitoylphosphatidylcholine (DPPC), and ovine brain GM1 were obtained from Avanti Polar Lipids; cholesterol and dihydrocholesterol (DChol) were obtained from Sigma. Fluorescein dihexadecanoyl phosphoethanolamine (F-DHPE), which partitions preferentially among the phases, thereby providing contrast, was obtained from Molecular Probes. Many experiments used DChol instead of cholesterol to minimize cholesterol oxidation. All critical experiments were repeated with cholesterol on an Ar-saturated subphase and in a chamber flooded with Ar gas. The phase behavior and other physical properties of the two sterols in mixtures with phospholipids are very similar (29, 31). We use the symbol DChol only when referring to a specific experiment employing this sterol.

Lipid mixtures with 0.5–1 mol % F-DHPE were spread from a 1-mg/ml chloroform solution on the air–water interface of a Teflon trough with a movable barrier to vary the surface pressure. The monolayer was observed by using epifluorescence microscopy and methods described previously (8). All experiments were carried out at room temperature on a subphase of PBS at pH 7.0. The CT-B subunit was labeled with Alexa Fluor 594 (Alexa) by using a labeling kit (Molecular Probes) yielding a final concentration of 0.59 mg/ml with 3.6 dye molecules/protein. The labeled protein was introduced into the subphase beneath the monolayer, and staining of the monolayer typically occurred 30–45 min later. Separate filters for F-DHPE and Alexa enabled independent observation of both dyes in the monolayer. β-cyclodextrin (β-CD) is a cyclic polysaccharide with a hydrophobic cavity that extracts cholesterol and DChol from monolayers and bilayers (29). In cholesterol or DChol extraction experiments, a 2-mM solution of β-CD was added to the subphase of the monolayer, and the surface pressure was kept constant during the course of sterol depletion by means of a movable barrier on the Teflon trough.

Results

Theoretical Pressure-Composition Phase Diagrams. Fig. 1*A–C* shows theoretical phase diagrams representative of experimental data for mixtures of cholesterol (or DChol) and various phospholipids. Binary mixtures of DChol and several phospholipids with unsaturated or short saturated fatty acid chains show a simple single two-phase immiscibility region as in Fig. 1*A* (30, 32). Binary mixtures of DChol (or cholesterol) and some phospholipids with long saturated fatty acid chains show two immiscibility regions, α and β, as in Fig. 1*B* (8, 30). In this phase diagram, the cusp occurs at the stoichiometry of the condensed complex. Phase diagrams of this type have also been reported for ternary mixtures of DChol (or cholesterol) and saturated phospholipids, indicating that they behave as pseudo binary mixtures (8). However, the phase rule allows the possibility of the simultaneous presence of three phases in such mixtures. This is illustrated by the calculated phase diagram in Fig. 1*C*, where α and β are two-phase regions and γ is a three-phase region. In previous work, we have described three distinct liquid phases in cholesterol-phospholipid monolayer mixtures: a phospholipid-rich phase, a condensed complex-rich phase, and a cholesterol-rich phase (9). However, in this earlier work, we were never able to detect unequivocally the simultaneous presence of three coexisting liquid phases. Model calculations described later point to the likely presence of regions with three coexisting phases, such as the γ region of Fig. 1*C*.

Experimental Phase Behavior. Fig. 1*D* shows an experimental outer boundary of a phase diagram of a DChol-lipid mixture where the nonsterol fraction contains 10% GM1 and a 1:1 molar ratio of egg-SM:DMPC. Similar phase transition pressures were obtained when cholesterol was used instead of DChol for several of the compositions. GM1 has been shown to be localized in raft domains in cell membranes, based on labeling with fluorescently labeled CT-B (28). This phase diagram is somewhat similar to that in Fig. 1*C*, suggesting the possibility of complex formation and three-phase coexistence. The observed domain morphology switches abruptly from α-like to β-like (7, 30) at a DChol mole fraction of $\approx$0.3. This rules out the possibility of a phase diagram such as in Fig. 1*A*.

Alexa-labeled CT-B was added to the subphase of a monolayer of the lipid mixture of Fig. 1*D* containing 30 mol % DChol and 1 mol % of F-DHPE. Fig. 2*A* shows an epifluorescence view of the monolayer excluding emission from the labeled CT-B. Very similar patterns have been observed for monolayers of the same composition without CT-B in the subphase. Also, the presence of CT-B in the subphase has no significant effect on the phase boundaries in Fig. 1*D*. Fig. 2*B* shows emission from the CT-B label, where the emission from F-DHPE is blocked. The same result was obtained when the experiment was repeated with cholesterol instead of DChol. From these and other similar observations it can be concluded that the monolayer is composed of three liquid phases—one that excludes both probes (F-DHPE and Alexa), another that accommodates one of the probes (F-DHPE) but not the other (Alexa), and a third that accommodates both probes (F-DHPE and Alexa). According to the thermodynamic model for condensed complexes, these phases are, in no particular order, a phospholipid-rich phase, a condensed complex-rich phase, and a cholesterol-rich phase.

Similar results have been obtained with two other lipid mixtures having phase diagrams similar to Fig. 1*B*. These mixtures contained 30% DChol and 7% GM1. In one case, the phospholipids were a 1:1 mixture of DMPC and DPPC. In the other case, the phospholipids were a 2:1 mixture of DMPS and DMPC. The experiments with the latter system were repeated with cholesterol, yielding the same results. In experiments on the DMPS-DMPC-GM1 mixture, the darkest domains were shown to be DChol-rich domains, based on DChol extraction with β-CD. When β-CD is included in the subphase of a monolayer of this mixture containing 30% DChol and the surface pressure is kept constant at 3 mN/m, the darkest domains (as viewed with both filters) become small relative to the other domains. This occurs well before the monolayer takes on the characteristics of a DChol-free monolayer when the low cholesterol mole fraction phase boundary of Fig. 1*B* is reached. Although the chemical activity of DChol is likely the same throughout the monolayer because of rapid lateral diffusion, the percentage of DChol in the

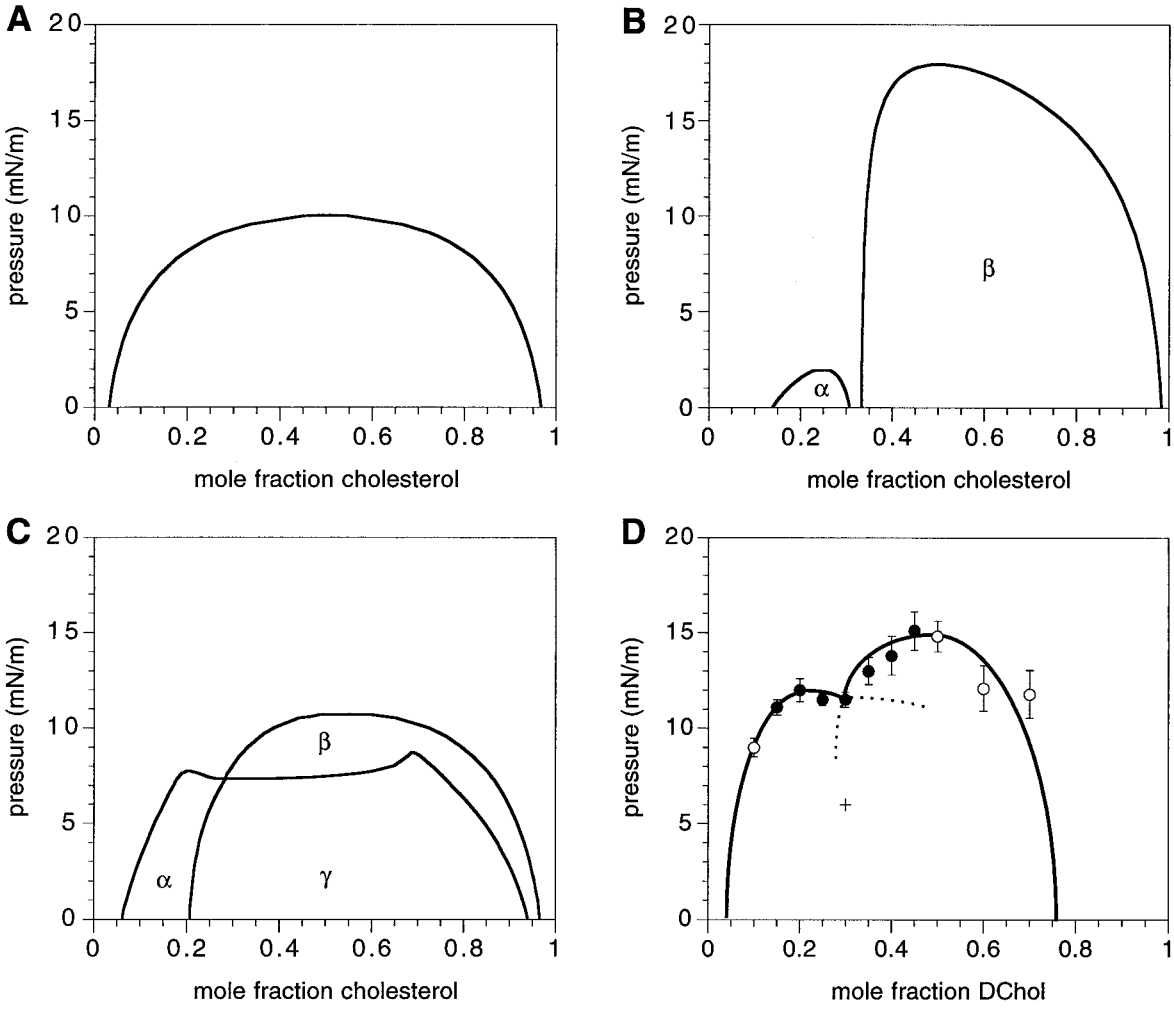

Fig. 1. (*A–C*) Calculated composition-pressure phase diagrams for mixtures containing cholesterol and one or more other lipids. (*A*) Binary mixture of cholesterol, C, with a non-complex-forming lipid U. (*B*) Binary mixture of C with a complex-forming lipid S. (*C*) Ternary mixture of C with U and S present in a 1:1 ratio. Regions of phase coexistence are identified as α, β, and γ. α and β are two-phase regions, and γ is a three-phase region. Compositions of coexisting phases were found by the method of double-tangent construction, using the free energy in Eq. **2** (28), with the parameters $p = 2$; $q = 1$; $n = 1$; $K^0_{eq} = 1{,}000$; $\Delta A = -40$ Å^2; $a_{SU} = 0$; $a'_{CS} = a'_{CU} = a'_{CX} = a'_{SX} = a'_{UX} = 1/6$; $\pi_{CS} = 12$ mN/m; $\pi_{CU} = 10$ mN/m; $\pi_{CX} = 18$ mN/m; $\pi_{SX} = 2$ mN/m; $\pi_{UX} = 9$ mN/m. "X" represents the complex $C_{nq}S_{np}$. (*D*) Experimental phase diagram showing liquid–liquid miscibility critical points for a mixture of DChol and phospholipids. The phospholipid fraction is a 1:1 molar mixture of egg-SM and DMPC along with 10% GM1. Plotted data points indicate transition pressures where phase coexistence disappears during monolayer compression. Above these pressures, there is a single uniform phase. Stripe superstructure phases, which are characteristic of proximity to a critical point, were observed at the transitions marked by ●. The sketched dotted lines illustrate the possibility of a three-phase region as in *C*. The "+" symbol represents pressure-composition conditions used in Fig. 2. The error bars represent deviations in three independent phase boundary measurements.

darkest phase is highest, so this phase tends to disappear first. Thus, the darkest domain, which excludes both fluorescent probes, is identified as the DChol- or cholesterol-rich phase.

Evidence that CT-B and hence GM1 are in the condensed complex-rich phase rather than the phospholipid-rich phase was obtained by studying mixtures where no complex is formed. In this case, there are only two phases present: a cholesterol-rich phase and a phospholipid-rich phase. Mixtures where no complex formation is observed, such as a binary mixture of DMPC and DChol, have phase diagrams as illustrated in Fig. 1*A* (30). At a pressure of 6 mN/m and 30% DChol, a DMPC-DChol monolayer with 1 mol % F-DHPE as a probe shows well-defined circular domains, often similar to those shown in Fig. 2*A*. The addition of 10% GM1 to this mixture does not change the domain morphology significantly. However, when Alexa-labeled CT-B is included in the subphase and the monolayer is then viewed with a light filter that blocks F-DHPE emission, there is no detectable fluorescence that could be attributed to the Alexa probe. From this experiment, we conclude that GM1 does not dissolve in either the phospholipid-rich or the DChol-rich domains. (GM1 presumably leaves the monolayer in micellar form). In general, GM1 may only be soluble in membranes favorable to condensed complex formation. Note that membrane solubility of GM1 does not require a phase-separated condensed complex domain; in the experiments shown in Fig. 2, GM1 remains in the membrane even as the membrane is made homogeneous by raising the pressure. Domains labeled with CT-B remain macroscopically liquid, so strong aggregation or crosslinking of the protein is ruled out. In conjunction with the β-CD experiments, this result shows that GM1 is in the condensed complex-rich phase of the three-phase mixture.

In some lipid mixtures containing DMPS and DMPC, the fluorescence contrast is the reverse of that seen in Fig. 2—black circular cholesterol-rich domains are observed in a monolayer sometimes surrounded by the condensed complex-rich phase (con-

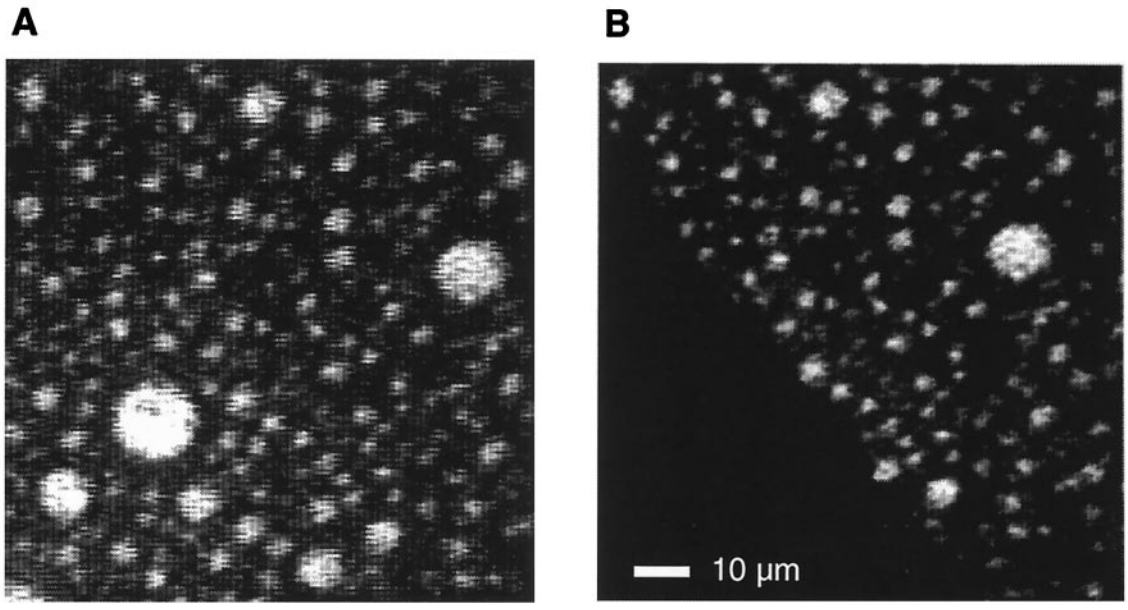

Fig. 2. Epifluorescence micrographs of a lipid monolayer containing 31% egg-SM, 31% DMPC, 7% GM1, 30% DChol, and 1% F-DHPE at a surface pressure of 6 mN/m. (The phase diagram of this mixture is shown in Fig. 1*D*, where the ''+'' symbol denotes the pressure-composition conditions used here.) The subphase contains Alexa-labeled CT-B. (*A*) View of the monolayer when observed with a F-DHPE-specific filter that excludes Alexa emission. (*B*) View of the same monolayer region when observed with an Alexa specific filter that excludes F-DHPE emission. When this monolayer is pressurized, all of the domains go through a critical phase transition at roughly the same pressure, suggestive of proximity to a tricritical point. The probe distribution demonstrates three coexisting phases.

taining GM1) and sometimes surrounded by the phospholipid-rich phase. Similar contrast reversal has been commonly observed in previous studies of monolayers with two coexisting liquid phases (33).

Ternary Phase Diagram. As noted in the introduction, we have extended the previous liquid-state model (8, 10) to include three components: cholesterol (C), a reactive lipid (S) that reacts with C to form a complex, and an unreactive lipid (U). The parameters used for the model are similar to those used before for binary mixtures. An illustrative ternary phase diagram is shown in Fig. 3*A*. It will be seen that there are two one-phase regions, three two-phase regions, and one three-phase region. A black dot is placed in one of the two-phase regions. At this point, the two coexisting phases are a condensed complex-rich phase and a phospholipid-rich phase. If the proportion of cholesterol in the membrane is increased, one moves in the direction of arrow 1 and passes into the three-phase region. Likewise, starting from the black dot composition, if one increases the relative proportion of the phospholipid U (direction of arrow 2), one also moves into the three-phase region. In general, the chemical activity of cholesterol increases rapidly as the membrane composition approaches the three-phase boundary, as illustrated in Fig. 3 *B* and *C*. This means that increasing the mole fraction of cholesterol (arrow 1) or increasing the proportion of unreactive phospholipids (arrow 2) increases the cholesterol chemical activity. The details of these phase diagrams obviously depend on the parameters used. The parameters were chosen without prejudice from the range of parameters obtained earlier in studies of binary mixtures. No new parameters are needed to describe the three-phase coexistence.

In earlier work, Silvius *et al.* have used a triangular phase diagram to describe ternary bilayer mixtures containing cholesterol and different types of phospholipids (34, 35). It is plausible that our theoretical model will be applicable to their phase diagram, and that their experimental techniques may be applicable to bilayers of the mixtures described in the present study. Here, we do not use the term "liquid-ordered phase (l_o)" as both the condensed complex- and cholesterol-rich phases likely have properties described by this terminology.

Discussion

We find that CT-B binds to GM1 in lipid monolayers in which there are condensed complexes, but not to lipid monolayers where there are no condensed complexes. Lipid compositions reported to be responsible for the formation of rafts in cell membranes are similar to those we find to favor condensed complex formation in monolayers. The staining of GM1 in the condensed complex-rich phase in monolayers, and in rafts in cell membranes, provides additional evidence for a close relationship between these condensed complexes and rafts. It is to be emphasized that rafts and condensed complexes are distinct in the following sense. Rafts are usually imagined to be fluid lipid domains in cell membranes; condensed complexes may form such domains as a separate liquid phase. However, under some (possibly biological) conditions of pressure, temperature, or electric field, there may be no separate liquid phase even though condensed complexes are present. Thus, the absence of phase separated domains in a cell membrane does not imply the absence of condensed complexes.

Our calculations for monolayers provide a model for the liquid state of a membrane, but provide little information about the "structure" of the complexes; insofar as they are defined here, the complexes are qualitatively compatible with a number of earlier proposals (36–41). Even when the membrane has the stoichiometric composition, the complex forms a liquid phase, so a crystal-like structure is not expected. A liquid crystal or crystal-like structure with many defects might be appropriate. The sharpness of the cusp in some of the monolayer phase diagrams with two critical points shows that the cooperative unit *n* for complex formation is sometimes large, of the order of 5–10 (9). That is, there may be as many as 15–30 molecules in a complex. This does not correspond to raft size: a putative raft domain may comprise many hundreds of complexes, along with

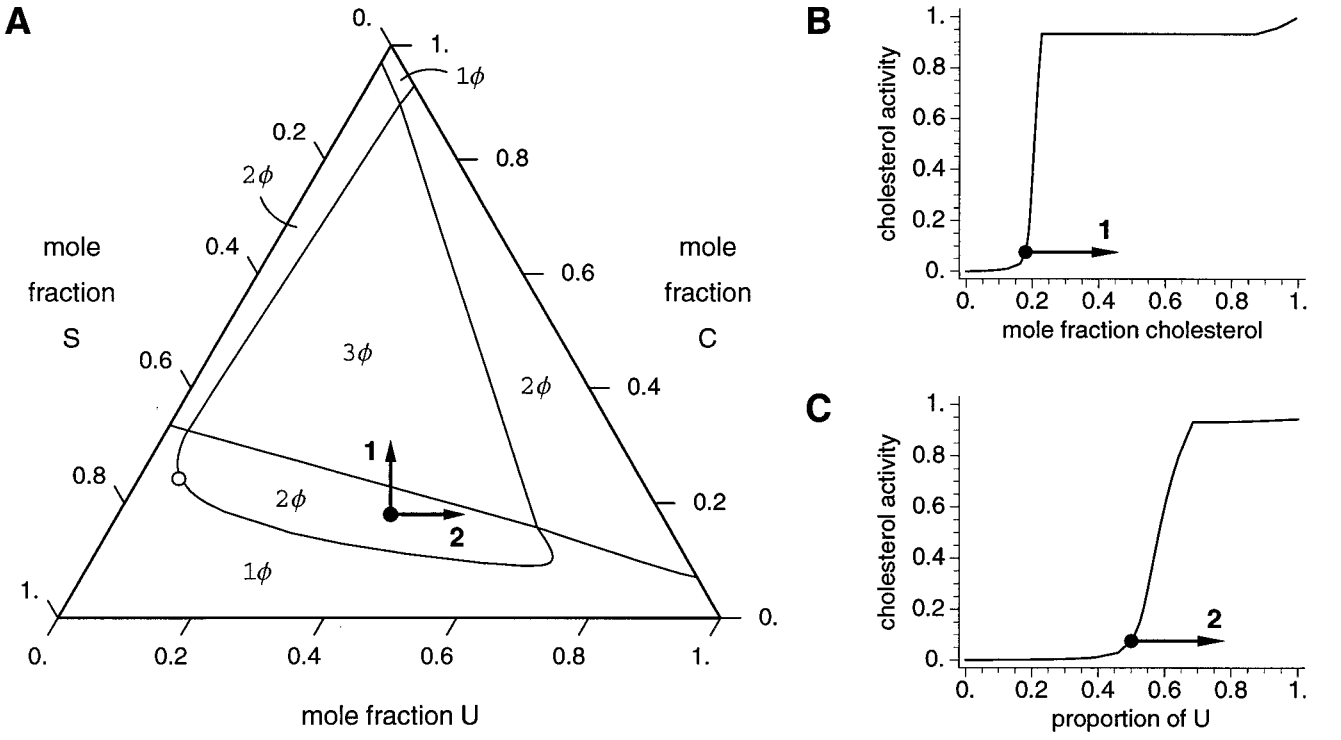

Fig. 3. (*A*) Calculated composition phase diagram for a ternary mixture of cholesterol C, with noncomplex-forming lipid U and complex-forming lipid S, using the same parameters as Fig. 1 *A–C*, for a surface pressure of $\pi = 4$ mN/m. Single-phase regions and regions of two- and three-phase coexistence are indicated by 1ϕ, 2ϕ, and 3ϕ, respectively. ○ indicates a critical point. The black dot denotes a mixture of 18% C and 41% each of S and U. Arrow 1 represents the addition of C to this mixture; arrow 2 represents an increase in the proportion of U in the nonsterol fraction. (*B*) Chemical activity of cholesterol as a function of cholesterol composition for a 1:1 mixture of S and U. (*C*) Chemical activity of cholesterol as a function of the proportion of U in the nonsterol fraction of a mixture containing 18% cholesterol. In *B* and *C*, the black dot indicates the composition of the mixture described in *A*; arrows 1 and 2 represent the composition changes described in *A*.

small amounts of uncomplexed lipids. The model parameters used for describing the phase diagrams for lipid monolayer mixtures will doubtless need to be modified for lipid bilayers. These parameters include the size, stoichiometry, and equilibrium constant of the complex. The monolayer experiments described here and in previous studies (8, 9) provide evidence for strong complex formation between cholesterol and sphingomyelin, and between cholesterol and phosphatidylserine. Thus, complex formation is to be expected on both the inner leaflet of a cell's plasma membrane, which contains cholesterol and phosphatidylserine, and on the outer leaflet, which contains cholesterol and sphingomyelin. It is plausible that complex formation is cooperative between both leaflets of the plasma bilayer. The ease with which intermolecular interactions may be varied in monolayers by changing molecular density provides clues, such as phase separations, for modeling that have thus far proved elusive in studies of bilayers.

The experiments and calculations reported here indicate how cholesterol–phospholipid complexes may have roles in animal cell membranes. The facilitation of raft formation in the plasma membrane is certainly one strong possibility. The lipid components of cell membranes would then be largely condensed complex, with the remainder composed of the more unsaturated phospholipids and possibly excess cholesterol. The condensed complexes might or might not form a separate phase. The regulation of the chemical activity of cholesterol is another likely function of complexes. If one imagines that the normal state of a plasma membrane corresponds to a point such as the black dot in Fig. 3*A*, then increasing cholesterol, decreasing sphingomyelin, or increasing the proportion of unsaturated phospholipids would all increase the cholesterol chemical activity. (There is considerable evidence that changing the concentration of cholesterol, sphingomyelin, or unsaturated phospholipids in cellular membranes affects the rate of cholesterol biosynthesis in these cells; refs. 42–46). As the composition of the membrane approaches the nearby three-phase boundary, the chemical activity of cholesterol rapidly increases. This should affect the binding of cholesterol to specific proteins in intracellular membranes, assuming intracellular lipid transport down the chemical activity gradient tends to maintain approximate equality of chemical activity throughout the cell. A rapid increase of cholesterol activity may also be associated with the formation of a cholesterol-rich (third) phase, which, in bilayers, could result in protein-mediated bleb and vesicle formation. Note, however, that phase separations are not required for rapid increases in chemical activity in the vicinity of the stoichiometric composition, as pointed out previously (29).

We thank Marija Vrljic for her help and advice in the protein labeling process. We are indebted to Robert Simoni for helpful discussions. This work was funded by the National Institutes of Health Grant 5R01 AI13587-25.

1. Feingold, L. (1993) *Cholesterol in Membrane Models* (CRC, Ann Arbor, MI).
2. Leathes, J. B. (1925) *Lancet* **208,** 853–856.
3. Albrecht, O., Gruler, H. & Sackmann, E. (1981) *J. Colloid Interface Sci.* **79,** 319–338.
4. Chapman, D. (1968) in *Membrane Models and the Formation of Biological Membranes*, eds. Bolis, L. & Pethica, B. A. (Interscience, New York), pp. 6–19.
5. Phillips, M. C. (1972) *Prog. Surf. Membr. Sci.* **5,** 139–221.
6. Müller-Landau, F. & Cadenhead, D. A. (1979) *Chem. Phys. Lipids* **25,** 315–328.

7. Radhakrishnan, A. & McConnell, H. M. (1999) *J. Am. Chem. Soc.* **121,** 486–487.
8. Radhakrishnan, A. & McConnell, H. M. (1999) *Biophys. J.* **77,** 1507–1517.
9. Radhakrishnan, A. & McConnell, H. M. (2000) *Proc. Natl. Acad. Sci. USA* **97,** 1073–1078.
10. Anderson, T. G. & McConnell, H. M. (2000) *Colloids Surf. A* **171,** 13–23.
11. Nielsen, M., Miao, L., Ipsen, J. H., Zuckermann, M. J. & Mouritsen, O. G. (1999) *Phys. Rev. E* **59,** 5790–5803.
12. Ipsen, J. H., Karlstrom, G., Mouritsen, O. G., Wennerstrom, H. & Zuckermann, M. J. (1987) *Biochim. Biophys. Acta* **905,** 162–172.
13. Slater, G. & Caille, A. (1981) *Phys. Lett. A* **86,** 256–258.
14. Corrales, L. R. & Wheeler, J. C. (1989) *J. Chem. Phys.* **91,** 7097–7112.
15. Talanquer, V. (1992) *J. Chem. Phys.* **96,** 5408–5421.
16. Simons, K. & Ikonen, E. (1997) *Nature (London)* **387,** 569–572.
17. Brown, D. A. & London, E. (1998) *Ann. Rev. Cell Dev. Biol.* **14,** 111–136.
18. Brown, R. E. (1998) *J. Cell Sci.* **111,** 1–9.
19. Hanada, K., Nishijama, M., Akamatsu, Y. & Pagano, R. E. (1995) *J. Biol. Chem.* **270,** 6254–6260.
20. Anderson, R. G. W. (1998) *Annu. Rev. Biochem.* **67,** 199–225.
21. Sheets, E. D., Holowka, D. & Baird, B. (1999) *Curr. Opin. Chem. Biol.* **3,** 95–99.
22. Okamoto, T., Schlegel, A., Scherer, P. E. & Lisanti, M. P. (1998) *J. Biol. Chem.* **273,** 5419–5422.
23. Viola, A., Schroeder, S., Sakakibara, Y. & Lanzavecchia, A. (1999) *Science* **283,** 680–682.
24. Simons, K. & van Meer, F. (1988) *Biochemistry* **27,** 6197–6202.
25. Brown, D. A. & Rose, J. K. (1992) *Cell* **68,** 533–544.
26. Bretscher, M. S. & Munro, S. (1993) *Science* **261,** 1280–1281.
27. Fielding, C. J. & Fielding, P. E. (1997) *J. Lipid Res.* **38,** 1503–1521.
28. Harder, T., Scheiffele, P., Verkade, P. & Simons, K. (1998) *J. Cell Biol.* **141,** 929–942.
29. Radhakrishnan, A. & McConnell, H. M. (2000) *Biochemistry* **39,** 8119–8124.
30. Keller, S. L., Radhakrishnan, A. & McConnell, H. M. (2000) *J. Phys. Chem. B* **104,** 7522–7527.
31. Benvegnu, D. J. & McConnell, H. M. (1993) *J. Phys. Chem.* **97,** 6686–6691.
32. Hagen, J. P. & McConnell, H. M. (1997) *Biochim. Biophys. Acta* **1329,** 7–11.
33. Keller, S. L. & McConnell, H. M. (1999) *Phys. Rev. Lett.* **82,** 1602–1605.
34. Silvius, J. R., del Giudice, D. & Lafleur, M. (1996) *Biochemistry* **35,** 15198–15208.
35. Brown, D. A. & London, E. (1998) *J. Membr. Biol.* **164,** 103–114.
36. Finean, J. B. (1953) *Experientia* **9,** 17–19.
37. Engelman, D. M. & Rothman, J. E. (1972) *J. Biol. Chem.* **247,** 3694–3697.
38. Gershfeld, N. L. (1978) *Biophys. J.* **22,** 469–488.
39. Parassassi, T., Giusti, A. M., Raimondi, M. & Gratton, E. (1995) *Biophys. J.* **68,** 1895–1902.
40. Presti, F. T., Pace, R. J. & Chan, S. I. (1982) *Biochemistry* **21,** 3831–3835.
41. Somerharju, P., Virtanen, J. A. & Cheng, K. H. (1999) *Biochim. Biophys. Acta* **1440,** 32–48.
42. Brown, M. S. & Goldstein, J. L. (1999) *Proc. Natl. Acad. Sci. USA* **96,** 11041–11048.
43. Lange, Y. & Steck, T. L. (1996) *Trends Cell Biol.* **6,** 205–208.
44. Scheek, S., Brown, M. S. & Goldstein, J. L. (1997) *Proc. Natl. Acad. Sci. USA* **94,** 11179–11183.
45. Lange, Y., Jin, Y., Rigney, M. & Steck, T. L. (1999) *J. Lipid Res.* **40,** 2264–2270.
46. Worgall, T. S., Sturley, S. L., Seo, T., Osborne, T. F. & Deckelbaum, R. J. (1998) *J. Biol. Chem.* **273,** 25537–25540.